

# blood

2005 105: 3663-3670  
Prepublished online Jan 18, 2005;  
doi:10.1182/blood-2004-08-3325

## Activity and specificity of toxin-related mouse T cell ecto-ADP-ribosyltransferase ART2.2 depends on its association with lipid rafts

Peter Bannas, Sahil Adriouch, Sarah Kahl, Fenja Braasch, Friedrich Haag and Friedrich Koch-Nolte

---

Updated information and services can be found at:  
<http://bloodjournal.hematologylibrary.org/cgi/content/full/105/9/3663>

Articles on similar topics may be found in the following *Blood* collections:  
[Immunobiology](#) (3873 articles)  
[Cell Adhesion and Motility](#) (790 articles)  
[Signal Transduction](#) (1930 articles)

---

Information about reproducing this article in parts or in its entirety may be found online at:  
[http://bloodjournal.hematologylibrary.org/misc/rights.dtl#repub\\_requests](http://bloodjournal.hematologylibrary.org/misc/rights.dtl#repub_requests)

Information about ordering reprints may be found online at:  
<http://bloodjournal.hematologylibrary.org/misc/rights.dtl#reprints>

Information about subscriptions and ASH membership may be found online at:  
<http://bloodjournal.hematologylibrary.org/subscriptions/index.dtl>



# Activity and specificity of toxin-related mouse T cell ecto-ADP-ribosyltransferase ART2.2 depends on its association with lipid rafts

Peter Bannas, Sahil Adriouch, Sarah Kahl, Fenja Braasch, Friedrich Haag, and Friedrich Koch-Nolte

**Adenosine diphosphate (ADP)-ribosyltransferases (ARTs) transfer ADP-ribose from nicotinamide adenine dinucleotide (NAD) onto target proteins. T cells express ART2.2, a toxin-related, glycosylphosphatidylinositol (GPI)-anchored ecto-enzyme. After the release of NAD from cells, ART2.2 ADP-ribosylates the P2X7 purinoceptor, lymphocyte function-associated antigen (LFA-1), and other membrane. Using lymphoma transfectants expressing either ART2.2 with its native GPI anchor (ART2.2-GPI) or ART2.2 with a grafted transmembrane anchor (ART2.2-Tm), we demonstrated that**

**ART2.2-GPI but not ART2.2-Tm associated with glycosphingolipid-enriched microdomains (lipid rafts). At limiting substrate concentrations, ART2.2-GPI exhibited more than 10-fold higher activity than ART2.2-Tm. On intact cells, ART2.2-GPI ADP-ribosylated a small number of distinct target proteins. Strikingly, the disruption of lipid rafts by cyclodextrin or membrane solubilization by Triton X-100 increased the spectrum of modified target proteins. However, ART2.2 itself was a prominent target for ADP-ribosylation only when GPI anchored. Furthermore, cholesterol depletion or detergent solubilization abolished**

**the auto-ADP-ribosylation of ART2.2. These findings imply that ART2.2-GPI, but not ART2.2-Tm, molecules are closely associated on the plasma membrane and lend support to the hypothesis that lipid rafts exist on living cells as platforms to which certain proteins are admitted and others are excluded. Our results further suggest that raft association focuses ART2.2 on specific targets that constitutively or inducibly associate with lipid rafts. (Blood. 2005;105:3663-3670)**

© 2005 by The American Society of Hematology

## Introduction

ART2.2 is a glycosylphosphatidylinositol (GPI)-anchored ecto-enzyme expressed on the surfaces of most terminally differentiated T cells.<sup>1</sup> ART2.2 is related in structure and function to adenosine diphosphate (ADP)-ribosylating bacterial toxins.<sup>2-4</sup> After the release of the ADP-ribosyltransferase (ART) substrate nicotinamide adenine dinucleotide (NAD) from cells by lytic or nonlytic mechanisms, ART2.2 catalyzes the transfer of ADP-ribose from NAD onto arginine residues onto leukocyte function-associated antigen (LFA-1), the P2X7 purinoceptor, and other cell-surface proteins.<sup>5,6</sup> Akin to protein phosphorylation, protein ADP-ribosylation usually profoundly affects the function of the modified target protein.<sup>7,8</sup> ADP-ribosylation activates P2X7, triggering calcium flux, phosphatidylserine flashing, and nonselective pore formation in the cell membrane.<sup>6</sup> ADP-ribosylation of LFA-1 and other cell-surface proteins inhibits the binding of T cells to target cells and interferes with the clustering of the T-cell receptor (TCR).<sup>5,9</sup>

Lipid rafts, also known as glycosphingolipid-enriched membranes (GEMs) or detergent-insoluble glycosphingolipid-enriched membranes (DIGs), are plasma membrane microdomains enriched in gangliosides and cholesterol that form liquid-ordered domains.<sup>10-12</sup> It is postulated that lipid rafts segregate molecules in the plasma membrane and regulate signaling through the spatial coordination of intermolecular interactions. Lipid rafts are characterized by insolubility in nonionic detergents and low buoyancy in sucrose density gradients. The posttranslational modification of proteins with saturated acyl groups can result in their localization

within lipid rafts. Thus, these microdomains are enriched in many signaling molecules, such as the Ick protein kinase, the adaptor protein LAT, heterotrimeric G proteins, and GPI-anchored proteins.<sup>13</sup> In addition, TCR and other transmembrane receptors, including interleukin-2 (IL-2) receptor and LFA-1, are inducibly recruited or stabilized in lipid rafts.<sup>14-16</sup> Activation of signaling molecules in lipid rafts is thought to facilitate signaling through the TCR and other immunoreceptors.<sup>17</sup>

Some cell-surface proteins lack a transmembrane-spanning domain and are anchored in the outer leaflet of the plasma membrane by a GPI moiety. The physiologic significance of the GPI anchor is unknown. Despite the fact that GPI-anchored proteins are restricted to the outer leaflet of the membrane lipid bilayer and lack a cytoplasmic domain, many GPI-anchored proteins can mediate signaling events after the binding of specific antibodies.<sup>18</sup> With Qa-2, CD55, and CD59, it has been shown that exchange of the GPI anchor by a transmembrane anchor abrogates antibody-induced signaling.<sup>19-21</sup> The association of GPI-anchored proteins with Src family kinases in lipid rafts may explain the involvement of GPI-anchored proteins in signaling.

Considering that ART2.2 and other members of the ART family carry a GPI anchor,<sup>22,23</sup> we hypothesized that the GPI anchor mediates lateral segregation of ART2.2 in rafts and that this might be a mechanism to regulate the activity and specificity of ART2. To test these hypotheses, we have adopted an experimental approach that has been successfully used in previous studies addressing the

From the Institute of Immunology, University Hospital, Hamburg, Germany.

Submitted August 26, 2004; accepted January 7, 2005. Prepublished online as *Blood* First Edition Paper, January 18, 2005; DOI 10.1182/blood-2004-08-3325.

Supported by grants SFB545-B9 and No310/6 from the Deutsche Forschungsgemeinschaft (F.H., F.K.-N.), the Fondation pour la Recherche Medical (S.A.), and the Werner Otto Foundation (P.B.).

**Reprints:** Friedrich Koch-Nolte, Institute of Immunology, University Hospital, Martinistr 52, D-20246 Hamburg, Germany; e-mail: nolte@uke.uni-hamburg.de.

The publication costs of this article were defrayed in part by page charge payment. Therefore, and solely to indicate this fact, this article is hereby marked "advertisement" in accordance with 18 U.S.C. section 1734.

© 2005 by The American Society of Hematology

lateral segregation of cell-surface enzymes in membrane microdomains. By replacing the native transmembrane anchors of angiotensin-converting enzyme (ACE) or  $\beta$ -secretase by a GPI anchor, Parkin et al<sup>24</sup> and Cordy et al<sup>25</sup> successfully sequestered the enzymes in lipid rafts. In this study, we used the mirror image approach and have replaced the native GPI anchor of ART2.2 with the transmembrane and cytosolic domains of CD8. Our results, indeed, indicate that sequestration within lipid rafts controls the activity and specificity of ART2.

## Materials and methods

### Materials

AEBSF (4-(2-aminoethyl)benzenesulfonyl fluoride), etheno-NAD, G418, and cholera toxin B subunit (CT) were obtained from Sigma Chemical (Deisenhofen, Germany). Monoclonal antibodies (mAbs) used in this study for immunofluorescence staining and immunoprecipitation include anti-FLAG (M2), anti-ART2.2 (AliA53), anti-LFA-1 (M17/4), and anti-etheno-adenosine 1G4. Phycoerythrin (PE)- and fluorescein isothiocyanate (FITC)-conjugated antibodies were purchased from PharMingen/Becton Dickinson (Heidelberg, Germany). Anti-ART2.2 AliA53 and P2X7-specific antiserum K1G were raised by gene-gun immunization, as described previously.<sup>1,6</sup> Antibodies were purified by affinity chromatography on Protein G Sepharose (Amersham-Pharmacia, Braunschweig, Germany) and were conjugated to fluorochrome Alexa488 according to the manufacturer's instructions (Molecular Probes, Eugene, OR). Anti-ART2.2-specific mAbs 9-13 and 10-6 (rat immunoglobulin G2a [IgG2a]) were kindly provided by Dr Lucienne Chatenoud (Paris, France). Anti-G $\beta$  polyclonal antibody (pAb T20) was purchased from Santa Cruz Biotechnology (Santa Cruz, CA).

### Cells and generation of ART2.2 transfectants

The mouse lymphoma cell line DC27.10 was kindly provided by Dr Bernhard Fleischer (Hamburg, Germany).<sup>26</sup> Vectors for expressing mouse ART2.2 in mammalian cells were cloned as described previously, replacing sequences for the N-terminal leader or the C-terminal GPI signal sequence.<sup>1</sup> Expression constructs were transfected into DC27.10 cells by electroporation (250 mV, 900  $\mu$ F) using 10  $\mu$ g DNA/ $10^7$  cells in 700  $\mu$ L RPMI and a Gene pulser (Bio-Rad GmbH, München, Germany). Stable transfectants were obtained by selection in medium supplemented with G418 (1 mg/mL). Cells were subcloned by limiting dilution, and clones were analyzed for ART2.2 expression levels by fluorescence-activated cell sorter (FACS) analysis.

### FACS analysis and immunocytochemistry

Cells ( $5 \times 10^5/100 \mu$ L) were incubated with or without phosphatidylinositol-specific phospholipase C (PI-PLC; Molecular Probes; 0.01 U/mL in [phosphate-buffered saline] PBS) for 1 hour at 37°C. For extraction of membrane proteins, cells were incubated in PBS containing 1% Triton-X-100 (TX-100) at 4°C for 10 minutes, diluted 10-fold in ice-cold PBS, 2% phosphonoformic acid (PFA), and fixed at 4°C for 30 minutes. Cells were stained with fluorochrome-conjugated antibodies and analyzed by flow cytometry on a FACSCalibur using CellQuest software (Becton Dickinson, Heidelberg, Germany), as described previously.<sup>1</sup> Dead cells were excluded after staining with propidium iodide. For immunocytochemistry, stained and fixed cells were centrifuged onto microscope slides using a cytospin centrifuge and mounted in fluorescence mounting medium (DAKO, Hamburg, Germany). Cells were visualized using a Leica (Wetzlar, Germany) confocal DM LFS microscope with a 40 $\times$  oil-immersion objective lens (numerical aperture 1.25) and Leica confocal software.

### Incubation of cells with etheno-NAD and staining with 1G4

Cells ( $1 \times 10^6$ ) were incubated with the indicated concentrations of etheno-NAD in 100  $\mu$ L RPMI medium for the indicated times at 37°C.

Cells were diluted 20-fold in medium and were washed twice. This was followed by incubation with Alexa488-1G4 (1  $\mu$ g/mL) or control antibodies for 30 minutes at 4°C. Cells were then analyzed by flow cytometry, as described previously.<sup>27</sup>

### Isolation of lipid rafts by density gradient centrifugation

Cells ( $2 \times 10^7$ ) were resuspended in 1 mL ice-cold lysis buffer (25 mM morpholinoethanesulfonic acid [MES], 150 mM NaCl, 5 mM EDTA [ethylenediaminetetraacetic acid], 1 mM AEBSF, 1% TX-100) at 4°C for 30 minutes. This was followed by 6 pulses (5 seconds) of ultrasonication (MSE ultrasonic disintegrator, low-power setting; MSE Scientific Instruments, Sussex, United Kingdom). An equal volume of an 80% sucrose solution (in lysis buffer) was mixed with the lysate, and a step gradient was formed by overlay with 6 mL of 30% sucrose and 4 mL of 5% sucrose. Isopycnic equilibration was achieved by centrifugation at 200 000g for 14 hours in a SW40 rotor (Beckman-Coulter, Krefeld, Germany) at 4°C. Twelve fractions (1 mL) were harvested from the top. Aliquots of each fraction (400  $\mu$ L) or from pooled fractions were acetone precipitated and subjected to Western blot analysis with the indicated antibodies. The pellet from the sucrose density gradients was dissolved directly in 2% sodium dodecyl sulfate (SDS; 100  $\mu$ L), and a 5- $\mu$ L aliquot was used for SDS-polyacrylamide gel electrophoresis (SDS-PAGE).

### Cell solubilization, immunoprecipitation, SDS-PAGE, and Western blot analysis

Cells were incubated in RPMI with or without etheno-NAD (1-50  $\mu$ M) or with 1  $\mu$ M <sup>32</sup>P-NAD (5  $\mu$ Ci [0.185 MBq]) for 10 minutes at 37°C. Cells were washed and resuspended in ice-cold lysis buffer ( $1 \times 10^7$  cells/mL PBS containing 0.05% or 1% TX-100, 1 mM AEBSF). After solubilization for 5 minutes at 4°C, insoluble material was removed by centrifugation (5 minutes, 500g, 4°C). The supernatant was collected (4°C lysate). Pellets were resuspended in prewarmed (37°C) lysis buffer and incubated for 20 minutes at 37°C. Insoluble material was removed by centrifugation (10 minutes, 500g, room temperature). The supernatant was collected (37°C lysate). Pellets were resuspended in PBS and 2% SDS and were solubilized on ice by 2 pulses (10 seconds) of ultrasonication (Bender ultra; high-power setting). For immunoprecipitation, anti-P2X7 antiserum K1G was conjugated to Aminolink matrix (Pierce, Rockford, IL) according to the manufacturer's instructions. Anti-LFA-1 mAb M17/4 was immobilized on Protein G Sepharose (Amersham-Pharmacia) (1  $\mu$ g/10  $\mu$ L beads). Lysates were cleared by high-speed centrifugation (15 minutes 15 000g) followed by incubation with Protein G Sepharose for 60 minutes at 4°C. Cleared lysates were incubated with immobilized antibodies (100  $\mu$ L lysate/10  $\mu$ L beads) for 60 minutes at 4°C. Immunoprecipitates were washed 5 times in lysis buffer. Bound material was eluted by heating in SDS-PAGE sample buffer for 10 minutes at 70°C. Proteins were size fractionated by electrophoresis on precast gels (Novex, Heidelberg, Germany) and blotted onto nitrocellulose (Hybond-N; Amersham-Pharmacia) or polyvinylidene difluoride (PVDF) (Immobilon; Applied Biosystems, Foster City, CA) membranes, as described previously.<sup>28</sup> Radioactivity incorporated into proteins was visualized by exposure of blots to Kodak X-Omat (Eastman Kodak, Rochester, NY) film for 24 hours at -80°C.

For immunoblot analysis, PVDF membranes were blocked with 5% dry milk (Nestle, Vevey, Switzerland), and proteins on the blots were detected by specific antibodies and the enhanced chemiluminescence (ECL) system (Amersham, Braunschweig, Germany). Blots were first probed with mAb 1G4 (0.5  $\mu$ g/mL in Tris-buffered saline [TBS], 1% dry milk, 0.05% Tween-20) and peroxidase-conjugated goat anti-mouse IgG. Subsequently blots were stripped with Re-Blot Plus stripping solution (Chemicon, Temecula, CA) and were probed with peroxidase-conjugated mAb M2 and peroxidase-conjugated CT. Blots were stripped again and probed further with pAb T20 and peroxidase-conjugated anti-rabbit IgG. Quantification of labeled bands was performed by densitometric scanning analysis using the AIDA 2.11 software (Raytest, Straubenhardt, Germany).

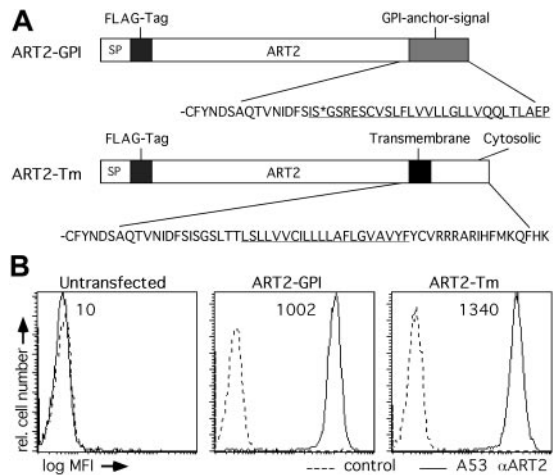


**Figure 1. Schematic diagram of wild-type ART2.2-GPI and ART2.2-Tm and stable expression of ART2.2-GPI and ART2.2-Tm by DC27.10 lymphoma cells.** (A) Domain structures of GPI-anchored ART2.2 (ART-GPI) and transmembrane-anchored ART2.2 (ART2.2-Tm) are shown. The N-terminal signal peptide of ART2.2 was replaced by the signal peptide of CD8 (SP) followed by a FLAG-tag. The wild-type GPI signal sequence of ART2.2-GPI is underlined, and the predicted GPI anchor attachment site is indicated by the asterisk. In the ART2.2-Tm construct, the C-terminal GPI anchor signal sequence was replaced by the 21-residue transmembrane domain of CD8 (underlined) and 5 flanking extracellular and 17 cytosolic amino acid residues. (B) DC27.10 lymphoma cells were stably transfected with ART2.2-GPI or ART2.2-Tm. Stable transfectants were selected by growth in the presence of G418 and subcloned by limiting dilution. Solid lines indicate levels of ART2.2 expression on the surfaces of parental untransfected lymphoma cells and of ART2.2-transfectants, determined by FACS analysis after staining with Alexa488-conjugated ART2.2-specific mAb AliA53. Dashed lines indicate cells treated with Alexa488-conjugated isotype control mAb. Numbers indicate mean fluorescence intensity (MFI) of ART2.2 staining.

## Results

### Expression of ART2.2-GPI and ART2.2-Tm in DC27.10

DC27.10 mouse lymphoma cells, which do not express detectable levels of ART2, were stably transfected with cDNA encoding GPI-anchored ART2.2 or ART2.2-Tm in which the GPI signal sequence was replaced with the distal juxtamembrane stalk, the transmembrane domain, and the cytoplasmic tail of CD8 (Figure 1A). Each construct was epitope tagged at the N-terminus with a FLAG-tag. FACS analysis with ART2.2-specific-mAb AliA53 and

FLAG-tag-specific mAb M2 confirmed cell-surface expression of each construct. Stable transfectants were selected and subcloned by limiting dilution. Subclones were tested for level of cell-surface ART2.2 expression, and clones with intermediate but similar expression levels were selected for further analyses (Figure 1B). Lysates from untransfected and ART2.2-transfected cells were subjected to immunoblot analyses with ART2.2-specific mAbs 9-13 and 10-6 or with anti-FLAG mAb M2. ART2.2-Tm migrated with a molecular weight of 45 kDa, whereas ART2.2-GPI migrated with an apparent molecular weight of 29 kDa.

### ART2.2-GPI but not ART2.2-Tm is released from cells by PI-PLC, whereas ART2.2-Tm but not ART2.2-GPI is released from cells by treatment with TX-100 at 4°C

GPI-anchored proteins can be released from the cell surface by treatment with bacterial PI-PLC, whereas transmembrane proteins are not affected by PI-PLC treatment.<sup>29</sup> Conversely, most transmembrane proteins can be released from the cell surface by treatment with the nonionic detergent Triton X-100 at 4°C, whereas GPI-anchored proteins are resistant to this treatment.<sup>30</sup> To confirm the nature of the membrane anchors of the ART2.2 constructs, ART2.2-transfected cells were treated with PI-PLC or TX-100 and then were subjected to FACS analyses with ART2.2-specific mAb AliA53. For control, cells were also stained for cell-surface expression of the type 1 transmembrane protein LFA-1 and for the raft marker GM1 (Figure 2A).

Treatment of cells with PI-PLC resulted in an 84% reduction of the cell-surface staining level for ART2.2-GPI (Figure 2A). In contrast, staining levels for ART2.2-Tm, LFA1, and GM1 were not affected by PI-PLC. Immunoblot analyses of cell supernatants from PI-PLC-treated cells confirmed that most ART2.2-GPI, but no detectable ART2.2-Tm, was released to the cell supernatant by treatment of cells with PI-PLC (Figure 3B, lanes 4-5).

Conversely, treatment of cells with TX-100 at 4°C led to a dramatic (97%-98%) reduction in cell-surface staining of ART2.2-Tm and LFA1 (Figure 2B). Similar results were obtained when cells were subjected to immunocytochemistry (Figure 2C). When the cells were incubated with 1% TX-100 at 4°C before fixation, the level of fluorescence in ART2.2-Tm-expressing cells was dramatically reduced (Figure 2Cviii), consistent with this construct residing in detergent-soluble regions of the plasma

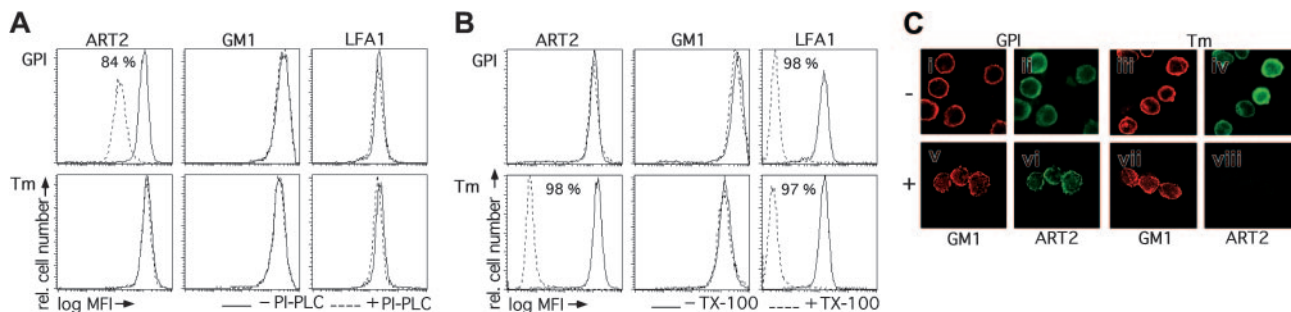


**Figure 2. ART2.2-GPI but not ART2.2-Tm is released from cells by exogenous PI-PLC treatment, whereas ART2.2-Tm but not ART2.2-GPI is released from cells by treatment with TX-100 at 4°C.** (A) DC27.10 cells stably transfected with ART2.2-GPI or ART2.2-Tm were incubated for 60 minutes at 37°C in the absence (solid lines) or presence (dashed lines) of PI-PLC. Cells were then washed and stained for cell-surface expression of GM1, ART2.2, or LFA-1 before FACS analysis. Number indicates the percentage reduction of the mean fluorescence intensity of PI-PLC treated compared with untreated ART2.2-GPI transfectants. (B) DC27.10 cells stably transfected with ART2.2-GPI or ART2.2-Tm were stained for cell-surface expression of GM1, ART2.2, or LFA1. Cells were then washed and incubated for 10 minutes at 4°C with or without 1% TX-100 before fixation and FACS analysis. Numbers indicate percentage reduction of mean fluorescence intensity of TX-100-treated compared with untreated cells. (C) DC27.10 cells stably transfected with ART2.2-GPI or ART2.2-Tm were stained for cell surface expression of GM1 and ART2. Cells were then washed and incubated for 10 minutes at 4°C with (+) or without (-) 1% TX-100 before fixation and confocal microscopic analysis. Results are representative of 3 independent experiments.

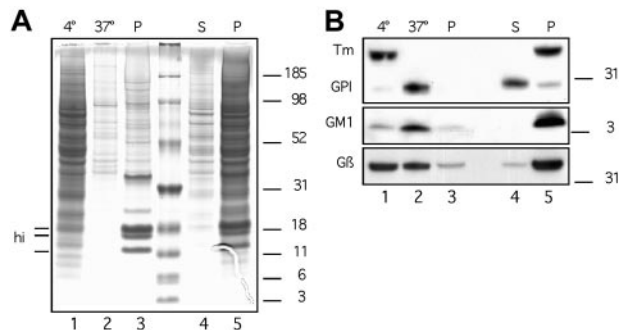


**Figure 3. Solubilization of ART2.2-GPI but not ART2.2-Tm by TX-100 is temperature sensitive.** DC27.10 cells stably transfected with ART2.2-GPI or ART2.2-Tm were pooled ( $1 \times 10^6$  of each cell type) and lysed in 1% TX-100 for 10 minutes at 4°C (lane 1). Insoluble material was pelleted by centrifugation and solubilized again in 1% TX-100 for 20 minutes at 37°C (lane 2). Insoluble material was pelleted by centrifugation. Pellets were solubilized by ultrasonication in 2% SDS (lane 3). A separate aliquot of pooled ART2.2-GPI- and ART2.2-Tm-transfected DC27.10 cells ( $1 \times 10^6$  of each) was incubated for 60 minutes with PI-PLC. PI-PLC-treated cells were pelleted by centrifugation, and the supernatant was collected (lane 4). The cell pellet was solubilized directly by ultrasonication in SDS (lane 5). Proteins were size fractionated by SDS-PAGE and stained with Coomassie brilliant blue (A). Histone bands in lane 3 are indicated (hi). An identical gel was subjected to immunoblot analysis (B). Immunodetection was performed sequentially by incubation of the blot with peroxidase (PO)-conjugated cholera toxin (GM1), PO-conjugated anti-FLAG mAb M2 (ART2-Tm and ART2-GPI), and rabbit antiserum T20 followed by PO-conjugated anti-rabbit IgG (Gβ). Results are representative of 3 independent experiments.

membrane. In contrast, ART2.2-GPI and GM1 retained punctuate staining patterns after pretreatment of cells with TX-100 (Figure 2Cv-vi), consistent with the localization of ART2.2-GPI in detergent-resistant rafts.

#### Differential segregation of ART2.2-Tm and ART2.2-GPI after a 2-step lysis protocol in Triton X-100

Although resistant to TX-100 solubilization at 4°C, GPI-anchored proteins reportedly can be solubilized by TX-100 at 37°C.<sup>31,32</sup> To test the solubility of ART2.2-GPI and ART2.2-Tm by TX-100, we subjected cells to a 2-step lysis protocol in which cells were first lysed in TX-100 for 10 minutes at 4°C (Figure 3). Insoluble material was pelleted by centrifugation, and the supernatant (4°C lysate) was harvested for analysis. Pellets were resuspended in prewarmed TX-100 and were incubated for 20 minutes at 37°C. Insoluble material was again pelleted by centrifugation, and the supernatant (37°C lysate) was harvested for analysis. Proteins in TX-100-resistant pellets were solubilized by ultrasonication in SDS. Size fractionation of proteins by SDS-PAGE and staining for total protein (Figure 3A) revealed that the 4°C lysate contained most (more than 80%) of the cellular protein (lane 1), whereas the 37°C lysate contained less than 5% of total cell protein (lane 2). Histones appeared as prominent bands only in the TX-100-resistant pellet fraction (lane 3). Immunoblot analysis (Figure 3B) revealed that ART2.2-Tm was almost completely solubilized by TX-100 at 4°C, whereas little if any ART2.2-GPI was contained in the 4°C lysate (lane 1). ART2.2-GPI, however, was readily solubilized at 37°C (lane 2). The traditional raft marker GM1 behaved like ART2.2-GPI: little, if any, GM1 was solubilized by TX-100 at 4°C, whereas a prominent GM1 band was obtained in the 37°C lysate. The heterotrimeric G-protein β subunit segregated partially into the 4°C and 37°C lysates. On treatment of cells with PI-PLC, most of ART2.2-GPI was released into the cell supernatant (lane 4), whereas ART2.2-Tm, GM1, and Gβ were resistant to PI-PLC (lane 5).

#### GPI-anchored but not transmembrane-anchored ART2.2 associates with glycosphingolipid-enriched microdomains (lipid rafts)

To determine whether ART2.2-GPI segregated with lipid rafts, cells were solubilized by ultrasonication in TX-100 at 4°C, and lipid rafts were isolated by sucrose gradient centrifugation. The position of lipid rafts was evident by an opaque band at the 5%/30% sucrose interface and was confirmed by immunoblotting for GM1 (Figure 4A-B). Only a small portion of the solubilized proteins was present in this fraction (Figure 4C). Most cellular proteins were located in the high-density fraction 12 and pellet (P) of the sucrose gradient (Figure 4C). Similar to GM1, ART2.2-GPI was strongly enriched in fraction 4, whereas only a small portion of ART2.2-Tm was found in this fraction (Figure 4A-B). These results further support the notion that most of ART2.2-GPI was raft associated, whereas little if any ART2.2-Tm was raft associated.

#### GPI-anchored ART2.2 mediates faster and more efficient etheno-ADP-ribosylation of cell-surface proteins than ART2.2-Tm

Using etheno-NAD as substrate and mAb 1G4 specific for etheno-adenosine, (etheno)-ADP-ribosylation cell-surface proteins can be detected by flow cytometry.<sup>27</sup> After 10-minute incubation of cells with 50 μM etheno-NAD, ART2.2-GPI- and ART2.2-Tm-transfected cells showed similar labeling with 1G4, indicating that both forms of ART2.2 were enzymatically active (Figure 5A). Untransfected DC27.10 cells showed only background staining with 1G4, confirming that ART2.2 is required for ADP-ribosylation of cell-surface proteins. Dose-response analyses revealed a stronger incorporation of etheno-NAD by ART2.2-GPI-transfected cells than by ART2.2-Tm-transfected cells at low substrate concentrations (Figure 5B). Half-maximal staining was obtained with 1 μM etheno-NAD for ART2.2-GPI-transfected cells compared with 20 μM etheno-NAD for ART2.2-Tm transfectants. Similarly, kinetic analyses (Figure 5C) revealed faster etheno-ADP-ribosylation of cell-surface proteins by ART2.2-GPI-transfected cells than by ART2.2-Tm transfectants (half-maximal staining less than 1 minute vs more than 20 minutes).

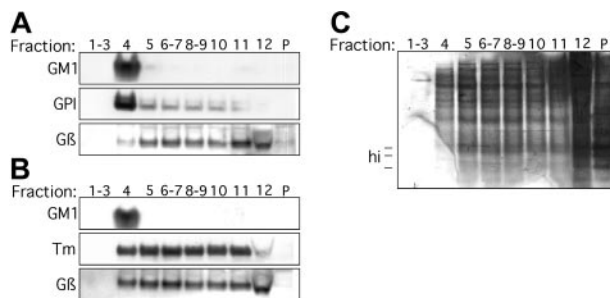


**Figure 4. ART2.2-GPI segregates with the lipid raft fraction in sucrose gradients.** DC27.10 cells stably transfected with ART2.2-GPI (A) or ART2.2-Tm (B) were solubilized by ultrasonication in 1% TX-100 at 4°C. Lysates were subjected to sucrose gradient centrifugation. Isopycnic equilibrium was achieved by centrifugation at 200 000g for 14 hours. Twelve fractions were harvested from the top of the gradient. Fractions 1-3, 6-7, and 8-9 were pooled. Fraction 4 contained the visible opaque band at the 5%/30% sucrose interface. The pellet at the bottom of the tube was resuspended by ultrasonication in 2% SDS. Proteins in individual or pooled fractions were precipitated and were subjected to SDS-PAGE immunoblot analysis using anti-ART2.2 mAbs 9-13/10-6, anti-Gβ, pAb, T20, and CT. Total protein in each fraction was visualized by silver staining (C). Results are representative of 3 independent experiments.

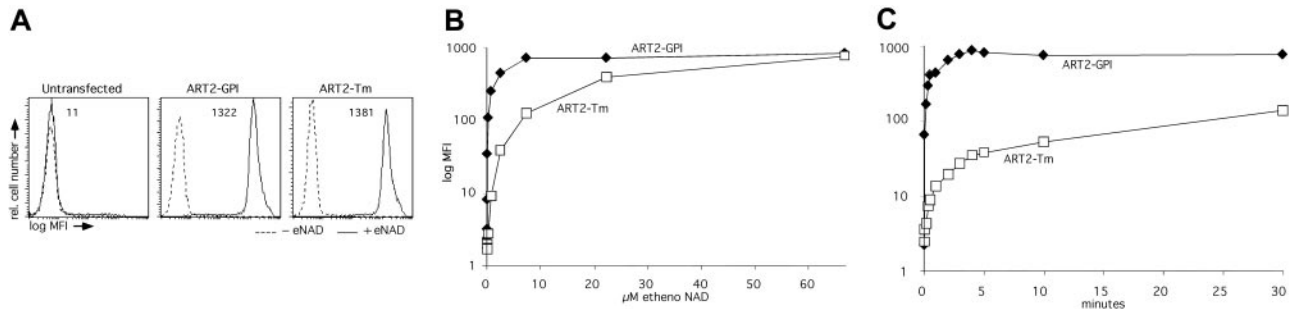


**Figure 5. Dose response and kinetics of etheno-ADP-ribosylation of cell-surface proteins by ART2.2-GPI- and ART2.2-Tm-transfected cells.** (A) Untransfected, ART2.2-GPI-transfected, and ART2.2-Tm-transfected DC27.10 cells were incubated for 10 minutes in the absence (dashed lines) or presence (solid lines) of 50  $\mu$ M etheno-NAD (eNAD). Cells were then washed, stained with Alexa488-conjugated mAb 1G4, and subjected to FACS analysis. Numbers indicate mean fluorescence intensity of cells incubated with etheno-NAD. (B) ART2.2-GPI-transfected ( $\blacklozenge$ ) or ART2.2-Tm-transfected ( $\square$ ) DC27.10 cells were incubated for 3 minutes in the presence of the indicated concentrations of etheno-NAD. Cells were then subjected to FACS analysis as in panel A. (C) ART2.2-GPI-transfected ( $\blacklozenge$ ) or ART2.2-Tm-transfected ( $\square$ ) DC27.10 cells were incubated for the indicated times in the presence of 1  $\mu$ M etheno-NAD. Cells were then subjected to FACS analysis as in panel A. Results are representative of 3 independent experiments.

### Disruption of lipid rafts by cyclodextrin inhibits cell-surface protein ADP-ribosylation catalyzed by ART2.2-GPI

To further investigate the influence of raft association on ART2.2 activity, we used an established protocol for disrupting lipid rafts on living cells, methyl- $\beta$ -cyclodextrin (MCD)-mediated extraction of cholesterol.<sup>33</sup> Pretreatment of cells with MCD, indeed, strongly inhibited the incorporation of etheno-ADP-ribose by ART2.2-GPI-transfected cells but had no detectable effect on etheno-ADP-ribosylation catalyzed by ART2.2-Tm (Figure 6A). To determine whether MCD treatment affected the solubility of proteins in TX-100, cells treated with MCD were subjected to sequential lysis in TX-100 and immunoblot analysis. As shown in Figure 6B, pretreatment of cells with MCD markedly enhanced the solubility

of ART2.2-GPI, GM1, and G $\beta$  in TX-100 at 4°C in a dose-dependent manner, consistent with the disruption of rafts by MCD treatment. Densitometric analyses showed that only 14% of ART2.2-GPI was solubilized by TX-100 at 4°C in untreated cells, whereas 45% of ART2.2-GPI was solubilized in MCD-treated cells (Figure 6B, lanes 1 and 7).

Remarkably, MCD treatment also strongly affected the pattern of target proteins subjected to etheno-ADP-ribosylation by ART2.2-GPI (Figure 6C). Immunoblot analyses with mAb 1G4 revealed several prominent bands in untreated ART2-GPI transfectants after incubation with 1  $\mu$ M etheno-NAD (lanes 1, 2). 1G4 staining intensity of these bands was markedly reduced after MCD treatment, and additional etheno-ADP-ribosylation protein bands became visible (lanes 4, 5). Overall, the pattern of etheno-ADP-ribosylation bands was diffuse and lighter in MCD-treated cells than in untreated cells.

Note that the size of the prominent 29-kDa target protein band in the 37°C lysate of untreated cells corresponds to that of ART2.2-GPI (Figure 6C, lane 2). Immunoprecipitation confirmed that this band represented ART2.2-GPI after etheno-ADP-ribosylation (not shown). Note that ADP-ribosylated ART2.2-GPI was no longer detectable in the 37°C TX-100 lysates of MCD-treated cells (Figure 6C, lane 5). Evidently, MCD treatment of cells resulted in weaker labeling and increased solubility of ART2.2-GPI. This is consistent with *trans*-ADP-ribosylation of ART2.2-GPI occurring in intact lipid rafts, but not after disruption of rafts with MCD. A similar phenomenon was observed for other detergent-resistant, etheno-ADP-ribosylation bands in untreated compared with MCD-treated cells (Figure 6C, lane 2 vs lane 5). Note also that in case of ART2.2-Tm transfectants incubated with 1  $\mu$ M etheno-NAD, 1G4 immunoblot analyses do not reveal any detectable bands (Figure 6C, lanes 7-9), consistent with the notion that the label incorporated by ART2.2-Tm transfectants was distributed over many weakly labeled proteins rather than a few prominent targets.

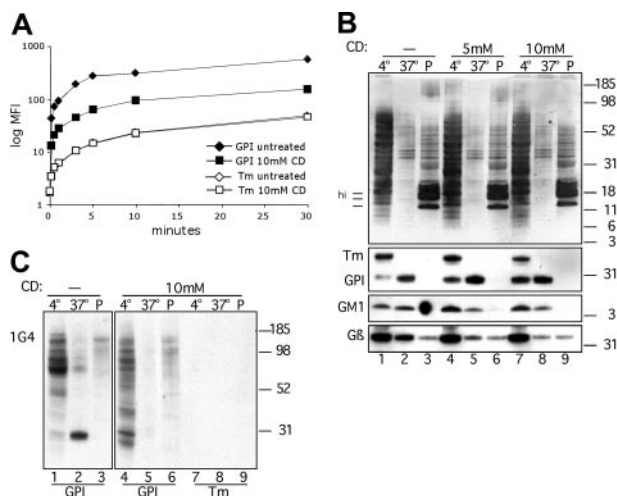


**Figure 6. Disruption of lipid rafts by  $\beta$ -MCD inhibits the activity of ART2.2-GPI.** (A) DC27.10 cells stably transfected with ART2.2-GPI (GPI; filled symbols) or ART2.2-Tm (Tm; open symbols) were incubated for 60 minutes in the absence (diamonds) or presence (squares) of 10 mM MCD. Cells were washed and incubated further in the presence of 1  $\mu$ M etheno-NAD for the indicated times. Cell-surface protein ADP-ribosylation was detected by FACS analysis with Alexa488-1G4, as in Figure 5. (B) Equal aliquots of ART2.2-GPI and ART2.2-TM cells were mixed and incubated for 60 minutes in the absence or presence of 5 to 10 mM MCD. Cells were then lysed in 2 steps in 1% TX-100, and proteins in cleared lysates were analyzed by immunoblot analysis, as in Figure 3. (C) Cells were incubated for 60 minutes in the absence or presence of 10 mM MCD. Cells were then washed and incubated further for 10 minutes in the presence of 1  $\mu$ M etheno-NAD. Immunodetection was performed by incubation of blots with mouse anti-etheno-adenosine mAb 1G4 followed by PO-conjugated anti-mouse IgG 1G4. Bound antibody was detected using ECL.

### Membrane compartmentalization restricts the specificity of target protein ADP-ribosylation by ART2

To further extend our findings, we performed comparative 1G4 immunoblot analysis of untransfected, ART2.2-GPI-transfected and ART2.2-Tm-transfected DC27.10 cells after incubation in the presence of low (1  $\mu$ M) (Figure 7A) and high substrate concentrations (50  $\mu$ M etheno-NAD) (Figure 7B). To monitor the TX-100 solubility of ART2.2 and its target proteins, cells were again lysed by the 2-step solubilization procedure. Control protein staining (not

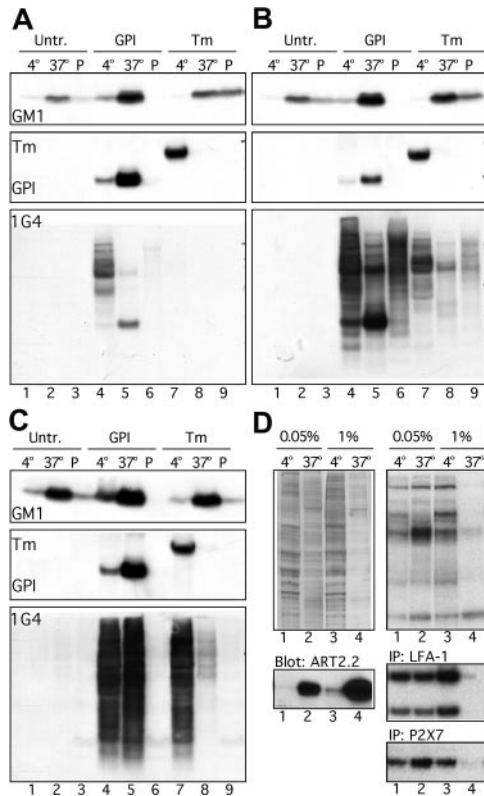


**Figure 7. Membrane compartmentalization restricts the specificity of target protein (etheno)-ADP-ribosylation by ART2.2.** (A-B) Untransfected (Untr.), ART2.2-GPI-transfected (GPI), and ART2.2-Tm-transfected (Tm) DC27.10 cells were incubated for 10 minutes in the presence of 1  $\mu$ M (A) or 50  $\mu$ M etheno-NAD (B). Cells were washed and then lysed in 2 steps in 1% TX-100 for 10 minutes at 4°C and then for 20 minutes at 37°C, as in Figure 3. TX-100-resistant pellets (P) were solubilized by sonication in 2% SDS. Proteins in cell lysates were acetone precipitated and subjected to size fractionation by SDS-PAGE, followed by Western blotting onto PVDF membranes. Immunodetection was performed as in Figure 6. (C) Cells were lysed by TX-100 and SDS, as described in panel B. Then 1  $\mu$ M etheno-NAD was added to each lysate, and lysates were incubated for 10 minutes at 37°C. Reactions were stopped by the addition of acetone, and proteins were analyzed by immunoblotting as in panel A. (D) ART2.2-GPI-transfected DC27.10 cells were incubated for 10 minutes in the presence of 1  $\mu$ M  $^{32}$ P-NAD. Cells were washed and lysed in 2 steps in 0.05% TX-100 (lanes 1, 2) or in 1% TX-100 (lanes 3, 4) for 10 minutes at 4°C and then in 1% TX-100 for 20 minutes at 37°C. Lysates were subjected to immunoprecipitation with immobilized anti-LFA-1 or anti-P2X7. Total protein in cell lysates was visualized by Coomassie brilliant blue staining, and ART2.2 was visualized by immunoblotting with PO-conjugated anti-FLAG mAb M2 (left panels). Radioactivity incorporated into proteins was determined by autoradiography; exposure times were 6 hours for LFA-1, 6 hours for total proteins, and 36 hours for P2X7 (right panels).

shown) and immunoblot analyses with CT and M2 (Figure 7, top panels) confirmed the segregation of type 1 membrane proteins in the 4°C lysates, GM1- and GPI-anchored proteins in the 37°C lysates, and nuclear proteins in the TX-100-resistant pellet (P). In accordance with the results of FACS analyses (Figure 5), labeling of target proteins was more efficient in ART2.2-GPI transfectants than in ART2.2-Tm transfectants. Note that in striking contrast to ART2.2-GPI, little if any ART2.2-Tm undergoes etheno-ADP-ribosylation (Figure 7A-B, lane 5 vs lane 7). Even at 50  $\mu$ M etheno-NAD, no labeling was observed in untransfected cells (Figure 7B, lanes 1-3), confirming that target protein etheno-ADP-ribosylation requires ART2.

Comparing the patterns of bands obtained with 1  $\mu$ M compared with 50  $\mu$ M etheno-NAD, ART2.2-GPI evidently labels a broader spectrum of bands at higher NAD concentrations (compare Figure 7A-B, lanes 4-6). Note that at high etheno-NAD concentrations, ART2.2-GPI and ART2.2-Tm apparently also label bands that are

resistant to TX-100 solubilization even at 37°C (Figure 7B, lanes 6 and 9).

We further compared the extent of ADP-ribosylation of LFA-1 and P2X7, 2 known target proteins of ART2.2,<sup>5,6</sup> after incubation of ART2.2-GPI and ART2.2-Tm transfectants with radiolabeled NAD. The results of immunoprecipitation analysis show that both proteins were modified more efficiently by ART2.2-GPI than by ART2.2-Tm (not shown). FACS analysis (not shown) revealed that P2X7 expression on DC27.10 cells was lower than on primary T cells, consistent with the relatively weak radiolabeling of P2X7 in Figure 7D compared with that by primary lymphocytes.<sup>6</sup> Note that both target proteins were efficiently solubilized at 4°C by 1% TX-100 (Figure 7D, lane 3). A substantial fraction of LFA-1 is associated with lipid rafts on EL4 and T28 mouse lymphoma cells, and the association of LFA-1 with lipid rafts is disrupted when cells are lysed with 1% TX-100 but not, or only partially, with 0.05% TX-100, which is thought to better preserve the integrity of lipid rafts.<sup>14-16</sup> Similarly, when DC27.10 cells were lysed with 0.05% TX-100, LFA-1, P2X7, and most other ADP-ribosylation proteins were found largely in the 37°C fraction (Figure 7D, lane 2). In contrast, most ART2.2-Tm (not shown) and most total protein were found in the 4°C fraction (Figure 7D) under these conditions.

#### Disruption of membrane integrity results in a dramatic increase in the extent of ART2.2-catalyzed protein ADP-ribosylation

To test whether association with the membrane restricts the access of ART2.2 to certain targets, we compared the ADP-ribosylation of target proteins on intact cells compared with cell lysates (Figure 7C). Indeed, when 1  $\mu$ M etheno-NAD was added to cell lysates rather than to intact cells, a dramatic (more than 50-fold) increase in the extent of protein etheno-ADP-ribosylation was observed (compare panels A and C in Figure 7). Promiscuous etheno-ADP-ribosylation was now observed for both ART2.2-GPI and ART2.2-Tm, even at this low etheno-NAD concentration. This implies that membrane association focuses ART2.2 onto specific targets.

## Discussion

Lipid rafts are thought to play an important role in mediating signal transduction through the cell membrane. Many lymphocyte ectoenzymes, including alkaline phosphatase, 5' nucleotidase, and ADP-ribosyltransferases, are GPI anchored.<sup>34</sup> Because the GPI anchor is thought to mediate raft association, it is conceivable that the sequestration within lipid rafts controls the activity of GPI-anchored ectoenzymes. Here we have addressed this hypothesis for T cell ecto-ADP-ribosyltransferase ART2.2 by exchanging its native GPI anchor with the transmembrane anchor of CD8, a classic type 1 membrane protein. In contrast to native ART2.2-GPI, ART2.2-Tm was insensitive to cleavage by PI-PLC (Figure 2) and showed little, if any, association with the lipid raft fraction on sucrose density gradient centrifugation (Figure 4). Moreover, in contrast to native ART2.2-GPI, ART2.2-Tm was readily solubilized by TX-100 at 4°C (Figures 2, 3). These results strongly suggest that ART2.2-GPI and ART2.2-Tm are associated with distinct membrane (micro)-domains.

The results of our solubilization assays are in accord with those of previous studies on the temperature-dependent solubilization of GPI-anchored-associated proteins by TX-100.<sup>31,32</sup> Filatov et al<sup>30</sup> showed that resistance of raft-associated proteins to solubilization by TX-100 at low temperature could be assessed by FACS analysis. Our results confirm this observation for ART2.2-GPI and extend it

to the classic raft marker asialo GM1 (Figure 2). Similarly, resistance of ART2.2-GPI and asialo GM1 to low-temperature detergent solubilization can be monitored by immunofluorescence microscopy (Figure 3B). Moreover, we show that despite its resistance to solubilization by TX-100 at 4°C, ART2.2-GPI is readily solubilized at 37°C (Figures 2, 3). Indeed, by treating cells sequentially with TX-100 first at 4°C and then at 37°C, GPI-anchored proteins and asialo GM1 could be separated from transmembrane-anchored proteins (Figure 3A). Therefore, differential solubilization of cells by TX-100 at 4°C compared with 37°C may provide a convenient and rapid evaluation of the possible association of membrane proteins and glycolipids with lipid rafts.

Interestingly, our results indicate that the lateral distribution of ART2.2 within the cell membrane dramatically affects its capacity to subject other cell-surface proteins to ADP-ribosylation. Using a recently established immunoassay for monitoring ART activity on living cells,<sup>27</sup> we found that both ART2.2-GPI and ART2.2-Tm could catalyze ADP-ribosylation of cell-surface proteins (Figure 5A). However, ADP-ribosylation catalyzed by ART2.2-GPI was much faster than that by ART2.2-Tm (Figure 5C). Moreover, ADP-ribosylation by ART2.2-GPI was more effective at lower—and presumably more physiologic—NAD concentrations than that by ART2.2-Tm (Figure 5B). Only at very high NAD concentrations and long incubation times did ADP-ribosylation reach similar levels of saturation for ART2.2-GPI- and ART2.2-Tm-transfected cells (Figure 5).

Steady state levels of extracellular NAD in biologic fluids (eg, serum) are in the submicromolar range, whereas intracellular NAD concentrations reach 200 to 500  $\mu\text{M}$ .<sup>35</sup> After lytic disruption of the plasma membrane, such as during tissue damage, hypoxia, or inflammation, local extracellular NAD concentrations can increase dramatically. Moreover, NAD reportedly can also be released nonlytically from some cells in a regulated manner through Connexin-43 hemichannels.<sup>36</sup> Extracellular NAD, however, is rapidly metabolized by ecto-NADases (such as CD38) and ectophosphodiesterases (such as PC-1).<sup>34</sup> Most likely, then, the relevant *in vivo* NAD concentrations and NAD exposure times are in a range (less than 10  $\mu\text{M}$ , less than 20 minutes) in which ART2.2-GPI shows more than 10-fold higher activity than ART2.2-Tm in lymphoma cells (Figure 5).

It has been proposed that GPI anchorage may influence lateral mobility within the cell membrane.<sup>37</sup> Our findings that ART2.2-GPI mediates cell-surface ADP-ribosylation with faster kinetics than ART2.2-Tm, but that both forms reach similar saturation levels at long incubation times, in principle, is consistent with a faster lateral mobility of ART2.2-GPI compared with ART2.2-Tm. Furthermore, it is conceivable that the length and flexibility of the juxtamembrane stalk affects access of ART2.2 to arginine residues in potential target proteins. In ART2.2-Tm, there are 20 amino acids between the hydrophobic transmembrane segment and the fourth conserved cysteine residue (which is engaged in a disulfide bond to the first cysteine in the 3-dimensional structure of rat ART2).<sup>4,38</sup> This corresponds to the distance from the cell membrane in ART2.2-GPI, encompassing the hydrophilic sugar residues of the GPI anchor and 16 amino acids between the site of the GPI anchor attachment on the first Ser residue in the Ser-Gly-Ser motif ( $\omega$ ,  $\omega + 1$ ,  $\omega + 2$ ) and the fourth conserved cysteine (Figure 1). The finding that known target proteins (LFA-1 and P2X7) can undergo ADP-ribosylation by both forms of ART2.2 (Figure 7) and the finding that both forms of ART2.2 reach similar saturation levels of cell-surface protein ADP-ribosylation at high NAD concentrations and long incubation times indicate that the observed striking differences in activity of ART2.2-GPI compared with ART2.2-Tm at low substrate concentra-

tions and short incubation times (Figure 5) are not caused by differences in the lengths of the juxtamembrane stalk.

Strikingly, when relieved from the restraint of the cell membrane, ART2.2-GPI and ART2.2-Tm show dramatically enhanced enzyme activities (Figure 6C), implying that membrane association restricts the accessibility of ART2.2 to certain targets. When in solution, ART2.2-GPI and ART2.2-Tm evidently are extremely promiscuous and effect ADP-ribosylation on numerous proteins. This is in accord with previous reports showing that soluble recombinant ART2.2 can effect ADP-ribosylation on many nonphysiologic targets, including histones, antibodies, and even free arginine.<sup>39</sup>

Moreover, the lateral distribution within the cell membrane, orchestrated by its membrane anchor, appears to further restrict the access of ART2.2 toward its targets. This interpretation is supported by the finding that the disruption of lipid rafts by MCD treatment alters the pattern of proteins that undergo ADP-ribosylation by ART2.2-GPI (Figure 6). In untreated cells, ART2.2-GPI modifies a small set of distinct target proteins. MCD-mediated depletion of cholesterol leads to a broader and more diffuse pattern of ADP-ribosylation target proteins (Figure 6C). Interestingly, 2 prominent targets of ART2-catalyzed ADP-ribosylation, LFA-1 and P2X7, at least partially localize to the raft fraction (Figure 7D), suggesting that raft association facilitates ADP-ribosylation of these target proteins. However, raft association of a particular protein alone is not sufficient for it to be targeted by ART2 (compare total vs radiolabeled protein bands in Figure 7D). Other unknown factors besides membrane composition must influence the ability of ART2 to target particular proteins. For example, the accessibility of arginine residues on a protein could determine whether it can undergo ADP-ribosylation. Moreover, surface loops adjacent to the NAD binding site of ART2 could confer target specificity, as was shown recently for exoenzyme S from *Pseudomonas aeruginosa*, the closest bacterial ART homolog, which, like ART2, can effect promiscuous ADP-ribosylation on many different targets.<sup>40,41</sup>

Given that much of the evidence for the existence and function of rafts has relied on biochemical analysis after detergent extraction rather than on studies with living cells, there has been considerable recent debate concerning the presence and size of rafts in living cells.<sup>11,12,42</sup> Our results bear some relevance to this debate because they show that the activity and specificity of a cell-surface enzyme on living cells depends on the nature of its membrane anchor (Figure 5) and on the cholesterol content of the cell membrane (Figure 6). These results support the notion that membrane proteins, indeed, are sequestered by lipids in different (micro)-domains on the surfaces of living cells. In this context, it is important to note that ART2.2 itself is a prominent target for *trans* ADP-ribosylation only when it is GPI anchored on the surfaces of living cells but not when it is anchored by a transmembrane domain (Figures 6, 7). Furthermore, ADP-ribosylation of ART2.2 is markedly reduced after cholesterol depletion (Figure 6C) or detergent extraction (Figure 7). These findings imply that 2 or more ART2.2-GPI molecules are in close vicinity on the intact cell surface and lend support to the hypothesis that lipid rafts exist as platforms to which certain proteins are admitted and others are excluded.

On the basis of these observations, we propose that raft association provides a topologic isolation for native GPI-anchored ART2.2 and focuses this enzyme onto specific targets, such as resident raft proteins or proteins that become transiently associated with rafts. A large body of evidence indicates that rafts play an important role during T-cell activation, when rafts are thought to establish a signal transduction platform within the immunologic synapse between T cells and antigen-presenting cells. It is tempting

to speculate that ART2.2 responds to NAD released from the antigen-presenting cells or from lysed cells in an inflammatory environment and regulates the function and geography of raft-associated proteins through ADP-ribosylation.

## Acknowledgments

Parts of this work represent partial fulfillment of the requirements for the graduate thesis of P.B. at the University Hospital, Hamburg.

This study was designed and supervised by F.K.-N. and F.H. P.B. performed the experiments described in Figures 1 to 7A-C, and S.A. performed the experiment described in Figure 7D. S.K. cloned the ART2.2-Tm expression constructs. F.B. established the stably transfected cell lines and purified and conjugated the anti-etheno-adenosine, anti-ART2.2, and anti-P2X7 antibodies. P.B. and F.K.N. wrote the paper. We thank Gabriela Boia, ZMNH, Hamburg, for expert technical assistance with confocal microscopy. We thank S. Rothenburg, C. Krebs, M. Seman, and B. Fleischer for critical reading of the manuscript.

## References

- Koch-Nolte F, Duffy T, Nissen M, et al. A new monoclonal antibody detects a developmentally regulated mouse ecto-ADP-ribosyltransferase on T cells: subset distribution, inbred strain variation, and modulation upon T cell activation. *J Immunol*. 1999;163:6014-6022.
- Domenighini M, Rappuoli R. Three conserved consensus sequences identify the NAD-binding site of ADP-ribosylating enzymes, expressed by eukaryotes, bacteria and T-even bacteriophages. *Mol Microbiol*. 1996;21:667-674.
- Aktorics K, Just I. *Bacterial Protein Toxins*. Berlin, Germany: Springer-Verlag; 2000.
- Mueller-Dieckmann C, Ritter H, Haag F, Koch-Nolte F, Schulz G. Structure of the Ecto-ADP-ribosyl transferase ART2.2 from rat. *J Mol Biol*. 2002;322:687-696.
- Nemoto E, Yu Y, Dennert G. Cell surface ADP-ribosyltransferase regulates lymphocyte function-associated molecule-1 (LFA-1) function in T cells. *J Immunol*. 1996;157:3341-3349.
- Seman M, Adriouch S, Scheuplein F, et al. NAD-induced T cell death: ADP-ribosylation of cell surface proteins by ART2 activates the cytolytic P2X7 purinoceptor. *Immunity*. 2003;19:571-582.
- Corda D, Di Girolamo M. Functional aspects of protein mono-ADP-ribosylation. *EMBO J*. 2003;22:1953-1958.
- Seman M, Adriouch S, Haag F, Koch-Nolte F. Ecto-ADP-ribosyltransferases (ARTs): emerging actors in cell communication and signaling. *Curr Med Chem*. 2004;11:857-872.
- Liu ZX, Yu Y, Dennert G. A cell surface ADP-ribosyltransferase modulates T cell receptor association and signaling. *J Biol Chem*. 1999;274:17399-17401.
- Simons K, Toomre D. Lipid rafts and signal transduction. *Nat Rev Mol Cell Biol*. 2000;1:31-39.
- Pike LJ. Lipid rafts: heterogeneity on the high seas. *Biochem J*. 2004;378:281-292.
- Horejsi V, Zhang W, Schraven B. Transmembrane adaptor proteins: organizers of immunoreceptor signalling. *Nat Rev Immunol*. 2004;4:603-616.
- Horejsi V. The roles of membrane microdomains (rafts) in T cell activation. *Immunol Rev*. 2003;191:148-164.
- Janes PW, Ley SC, Magee AI. Aggregation of lipid rafts accompanies signaling via the T cell antigen receptor. *J Cell Biol*. 1999;147:447-461.
- Marmor MD, Julius M. Role for lipid rafts in regulating interleukin-2 receptor signaling. *Blood*. 2001;98:1489-1497.
- Marwali MR, Rey-Ladino J, Dreolini L, Shaw D, Takei F. Membrane cholesterol regulates LFA-1 function and lipid raft heterogeneity. *Blood*. 2003;102:215-222.
- Bromley SK, Burack WR, Johnson KG, et al. The immunological synapse. *Annu Rev Immunol*. 2001;19:375-396.
- Robinson PJ. Signal transduction via GPI-anchored membrane proteins. *Adv Exp Med Biol*. 1997;419:365-370.
- Robinson PJ, Millrain M, Antoniou J, Simpson E, Mellor AL. A glycosphospholipid anchor is required for Qa-2-mediated T cell activation. *Nature*. 1989;342:85-87.
- Shenoy-Scaria AM, Kwong J, Fujita T, Olszowy MW, Shaw AS, Lublin DM. Signal transduction through decay-accelerating factor: interaction of glycosyl-phosphatidylinositol anchor and protein tyrosine kinases p56lck and p59fyn 1. *J Immunol*. 1992;149:3535-3541.
- Su B, Wanek GL, Flavell RA, Bothwell AL. The glycosyl phosphatidylinositol anchor is critical for Ly-6A/E-mediated T cell activation. *J Cell Biol*. 1991;112:377-384.
- Okazaki IJ, Kim HJ, McElvaney NG, Lesma E, Moss J. Molecular characterization of a glycosylphosphatidylinositol-linked ADP-ribosyltransferase from lymphocytes. *Blood*. 1996;88:915-921.
- Glowacki G, Braren R, Firner K, et al. The family of toxin-related ecto-ADP-ribosyltransferases in humans and the mouse. *Protein Sci*. 2002;11:1657-1670.
- Parkin ET, Tan F, Skidgel RA, Turner AJ, Hooper NM. The ectodomain shedding of angiotensin-converting enzyme is independent of its localisation in lipid rafts. *J Cell Sci*. 2003;116:3079-3087.
- Cordy JM, Hussain I, Dingwall C, Hooper NM, Turner AJ. Exclusively targeting beta-secretase to lipid rafts by GPI-anchor addition up-regulates beta-site processing of the amyloid precursor protein. *Proc Natl Acad Sci U S A*. 2003;100:11735-11740.
- Gabert J, Langlet C, Zamoyska R, Parnes JR, Schmitt-Verhulst AM, Malissen B. Reconstitution of MHC class I specificity by transfer of the T cell receptor and *Lyt-2* genes. *Cell*. 1987;50:545-554.
- Krebs C, Koestner W, Nissen M, et al. Flow cytometric and immunoblot assays for cell surface ADP-ribosylation using a monoclonal antibody specific for ethenoadenosine. *Anal Biochem*. 2003;314:108-115.
- Kahl S, Nissen M, Girisch R, et al. Metalloprotease-mediated shedding of enzymatically active mouse ecto-ADP-ribosyltransferase ART2.2 upon T cell activation. *J Immunol*. 2000;165:4463-4469.
- Stiernberg J, Low MG, Flaherty L, Kincade PW. Removal of lymphocyte surface molecules with phosphatidylinositol-specific phospholipase C: effects on mitogen responses and evidence that ThB and certain Qa antigens are membrane-anchored via phosphatidylinositol. *J Immunol*. 1987;138:3877-3884.
- Filatov AV, Shmigol IB, Kuzin II, Sharonov GV, Feofanov AV. Resistance of cellular membrane antigens to solubilization with Triton X-100 as a marker of their association with lipid rafts—analysis by flow cytometry. *J Immunol Methods*. 2003;278:211-219.
- Cain TJ, Liu Y, Takizawa T, Robinson JM. Solubilization of glycosyl-phosphatidylinositol-anchored proteins in quiescent and stimulated neutrophils. *Biochim Biophys Acta*. 1995;1235:69-78.
- Thiele HG, Koch F, Hamann A, Arndt R. Biochemical characterization of the T-cell alloantigen RT-6.2. *Immunology*. 1986;59:195-201.
- Cherukuri A, Dykstra M, Pierce SK. Floating the raft hypothesis: lipid rafts play a role in immune cell activation. *Immunity*. 2001;14:657-660.
- Goding JW, Howard MC. Ecto-enzymes of lymphoid cells. *Immunol Rev*. 1998;161:5-10.
- Ziegler M. New functions of a long-known molecule: emerging roles of NAD in cellular signaling. *Eur J Biochem*. 2000;267:1550-1564.
- Bruzzone S, Guida L, Zocchi E, Franco L, De Flora A. Connexin 43 hemi channels mediate Ca<sup>2+</sup>-regulated transmembrane NAD<sup>+</sup> fluxes in intact cells. *FASEB J*. 2001;15:10-12.
- Zhang F, Crise B, Su B, et al. Lateral diffusion of membrane-spanning and glycosylphosphatidylinositol-linked proteins: toward establishing rules governing the lateral mobility of membrane proteins. *J Cell Biol*. 1991;115:75-84.
- Ritter H, Koch-Nolte F, Marquez VE, Schulz GE. Substrate binding and catalysis of ecto-ADP-ribosyltransferase 2.2 from rat. *Biochemistry*. 2003;42:10155-10162.
- Koch-Nolte F, Petersen D, Balasubramanian S, et al. Mouse T cell membrane proteins Rt6-1 and Rt6-2 are arginine/protein mono(ADP-ribose) transferases and share secondary structure motifs with ADP-ribosylating bacterial toxins. *J Biol Chem*. 1996;271:7686-7693.
- Koch-Nolte F, Reche P, Haag F, Bazan F. ADP-ribosyltransferases: plastic tools for inactivating protein and small molecular weight targets. *J Biotechnol*. 2001;92:81-87.
- Sun J, Maresso AW, Kim JJ, Barbieri JT. How bacterial ADP-ribosylating toxins recognize substrates. *Nat Struct Mol Biol*. 2004;11:868-876.
- Munro S. Lipid rafts: elusive or illusive? *Cell*. 2003;115:377-388.